HMG Advance Access published July 5, 2007

Cholesterol biosynthesis pathway is disturbed in YAC128 mice and is modulated by huntingtin mutation

Marta Valenza[1,§], Jeffrey B Carroll[2,§], Valerio Leoni[3], Lisa N. Bertram[2], Ingeman Björkhem[4], Roshni R. Singaraja[2], Stefano Di Donato[3], Dieter Lutjohann[5], Michael R. Hayden[2] and Elena Cattaneo[1,*]

[1]Department of Pharmacological Sciences and Centre for Stem Cell Research, University of Milan, Italy. [2] Centre for Molecular Medicine and Therapeutics, Department of Medical Genetics, University of British Columbia, Vancouver, Canada. [3] C. Besta Neurological Institute, Milan, Italy. [4] Division of Clinical Chemistry, Department of Laboratory Medicine, Karolinska University Hospital, Stockholm, Sweden. [5] Department of Clinical Pharmacology, University of Bonn, Germany

*Corresponding author: Elena Cattaneo, Department of Pharmacological Sciences and Centre for Stem Cell Research, University of Milan, Italy. Tel. (+39)-02-50318333; Fax (+39)-02-50318284; email: elena.cattaneo@unimi.it

[§]The authors wish it to be known that, in their opinion, the first two authors should be regarded as joint First Authors.

ABSTRACT

Our recent analyses of the cholesterol biosynthetic pathway in Huntington's disease (HD) cells, the R6/2 huntingtin-fragment mouse model of HD as well as in human tissues has provided the first evidence of altered activity of this pathway in genetically identifiable HD samples. Here we report that these changes also occur in the full-length-huntingtin YAC128 mouse model, which shows a consistent reduction in the activity or levels of multiple components of the cholesterogenic pathway. We also show that this phenotype is progressive and is specific for the brain region most affected in HD., Mice over-expressing the wild-type protein with 18 CAG (YAC18 mice) show the opposite phenotype with higher activity of the cholesterol biosynthetic pathway compared to littermate mice. Finally, we report that plasma levels of cholesterol, its precursors and its brain-derived catabolite 24-S-hydroxycholesterol in YAC mice mirror brain biosynthetic levels supporting further investigation of their potential as peripheral biomarkers in HD.

INTRODUCTION

Huntington's disease (HD) is a dominantly inherited neurodegenerative disorder caused by an expanded CAG trinucleotide repeat in the coding region of the HD gene (1). Mutations code for expanded glutamine tracts in huntingtin, a 348 kDa protein essential for embryogenesis (2, 3, 4) and endowed with neuroprotective activities (5). The classic neuropathological features of HD are neuronal intranuclear and cytoplasmic inclusions of huntingtin aggregates (6) and cell death, primarily in the striatum and cerebral cortex (7). The disease typically manifests in midlife and causes progressive motor, psychiatric and cognitive dysfunctions leading ultimately to death (8).

In 2002 we reported that the mRNA levels for key genes in the cholesterol biosynthetic pathway are diminished in mutant huntingtin inducible cells (9) and have subsequently shown that a similar reduction occurs in brain tissue from R6/2 huntingtin-fragment mice (10), *post-mortem* brain specimens from HD patients and in primary fibroblasts from HD patients (11). The underlying molecular mechanism is impaired nuclear translocation of sterol regulatory-element binging proteins (SREBPs), transcription factors that regulate the expression of key genes involved in cholesterol biosynthesis. This defect leads to reduced total sterol mass in HD tissues and impaired cholesterol biosynthesis in HD cells (11).

Modifications in cholesterol homeostasis in the brain significantly impact neuronal function. Most cholesterol in the Central Nervous System (CNS) derives from *in situ* synthesis (12) and it has roles in signal transduction, synaptogenesis and neurotrasmitter release (13). The critical glial-derived factor required for efficient synaptogenesis *in vitro* has been identified as cholesterol (14), and alterations in brain cholesterol homeostasis lead to neurological symptoms in mice and humans (15). Additionally, cholesterol depletion was found to protect cultured neurons from excitotoxic death caused by the glutamate receptor agonist N-methyl-D-aspartic (NMDA) (16), suggesting the existence of a possible link between cholesterol homeostasis and neurotransmitter receptor function

In the present study, we explored the evidence for cholesterol homeostasis alterations in the yeast artificial chromosome (YAC) mouse model of HD (YAC128; 17), which expresses full-length mutant human huntingtin under the control of endogenous regulatory elements. This model has been shown to accurately recapitulate many of the signs and symptoms of HD, including cognitive (18) motor and neuropathological defects (17, 18). We show that YAC128 mice have progressively reduced sterol levels in the striatum with respect to littermate (WT) and mice over-expressing full-length normal human huntingtin (YAC18; 19). Consistent with this deficit, cholesterol precursors as well as the activity of 3-hydroxy-methyl-glutaryl-CoA-Reductase (HMGCoAR), the rate limiting cholesterol biosynthetic enzyme, were decreased in brain of YAC128 mice, indicative of a decrease in cholesterol synthesis. 24-S-hydroxycholesterol (24OHC) is a brain-specific cholesterol metabolite that is a marker of brain cholesterol turnover and is detectable in blood (20). In agreement with the reduced cholesterol synthesis in brain, a progressive decrease in the brain and plasma levels of 24OHC is found in YAC128 mice. By contrast, YAC18 mice show higher levels of brain and plasma cholesterol, brain and plasma cholesterol precursors, 24OHC and increased brain HMGCoAR activity with respect to WT mice. This evidence suggests that the human huntingtin protein influences cholesterol biosynthesisand that cholesterol homeostasis is altered in YAC128 mice directly by the mutation in human huntingtin.

RESULTS

Total sterol levels are progressively reduced in the striatum of YAC128 mice

Tissues from HD patients, as well as R6/2 mice, demonstrate impaired cholesterol biosynthesis (11; Valenza et al., unpublished). In order to examine whether this phenotype was observable in the CNS of other mouse models we measured total sterols in the brains of WT, YAC128 and YAC18 mice. We used an enzymatic method that measures not only cholesterol, but also additional sterol species (21). Using this method we discovered that total sterols are reduced by 40% in the striatum of 10-month old YAC128 mice compared to WT and YAC18 mice (Fig. 1a, one-way ANOVA $p = 0.0004$). At 10 months of age the striatum of YAC128 mice shows significant atrophy, whereas cortical atrophy becomes apparent at 12 months (17). Cortical sterol levels in the 10-month old YAC128 were slightly decreased when compared to WT (13% decrease, Mann-Whitney $p > 0.05$) and YAC18 mice (16% decrease, Mann-Whitney $p < 0.05$). In contrast, cerebellar sterol levels from YAC128, WT and YAC18 mice were similar at 10 months of age (Fig. 1c).

Total striatal sterol levels in YAC128 and control mice at 2 and 18 months of age indicate that this dysfunction is progressive (Table 1). At 2 months of age the YAC128 mice show cognitive deficits (18) while striatal and cortical neuropathology appear later at 9 and 12 months of age respectively (17). Normally, sterols progressively accumulate during development in mouse brain, reaching stable levels in adult mice (13). Consistent with this, total sterols rose in the striatum of WT mice between 2-18 months by ~45%. Striatal sterol levels were normal in the YAC128 mice at 2 months of age, but were significantly decreased compared to WT littermates at 18 months (Table 1). Similar results were found in cortex: in 18-month old YAC128 mice cortical total sterol accumulation was slightly reduced compared to control mice, though significance was not reached ($p = 0.054$; Table 1), suggesting that sterol defects in cortical tissue may be present but appear at later stages.

Brain cholesterol biosynthesis is reduced in YAC128 mice but increased in YAC18 mice

In order to address the mechanism underlying the observed sterol deficits in YAC128 mice, we applied isotopic-dilution mass spectrometry (MS) to discriminate between the levels of cholesterol and its precursors (see figure 2a – brief scheme of the cholesterol biosynthetic pathway). The level of lathosterol, the precursor of cholesterol whose production is catalyzed by the enzyme Δ8, Δ7 isomerase, is considered an indicator for cholesterol *neo*-genesis (22) and its reduction indicates that cholesterol biosynthesis is reduced in a given tissue.

We analyzed lathosterol levels in 2-month old YAC128 mice. Isotopic-dilution mass spectrometry showed that lathosterol levels are reduced by ~23% in 2-month old YAC128 mice compared to WT mice ($p=0.03$; figure 2b). At this time point total sterols as measured by enzymatic methods are not decreased in YAC128 mice (see table 1), but lathosterol levels are on the scale of 25ng/mg of tissue – or approximately 0.1% of total sterols. It is not surprising therefore that total sterol measurements do not allow discrimination of the observed differences in lathosterol.

Lathosterol levels were more significantly reduced, by ~38%, in total brain from 10-month old YAC128 mice compared to WT mice ($p = 0.013$) (figure 2c). By contrast, 10-month old YAC18 mice had lathosterol levels ~30% higher than WT mice ($p = 0.010$) and ~56% higher thanYAC128 mice ($p < 0.001$). We also measured other key cholesterol precursors, such as lanosterol and desmosterol (see figure 2a). At 2 months of age lanosterol but not desmosterol, was significantly reduced (figure 3, a and c; $p=0.05$) while at 10 months of age, both lanosterol and desmosterol were significantly reduced as previously observed for lathosterol (figure 3b and d).

Cholesterol levels in the whole brain of YAC128, YAC18 and WT mice were also examined by MS. At two months of age, there was no difference in brain cholesterol levels between YAC128 and WT mice (figure 3e). By 10 months of age, however YAC128 mice have significantly decreased total brain cholesterol when compared to WT (~17%, $p < 0.05$) and YAC18

mice (~26%, $p < 0.05$). In contrast, YAC18 mice have increased whole brain cholesterol with respect to WT and YAC128 mice, which only reached significance when compared to YAC128 mice ($p < 0.05$). The observed trends in whole brain cholesterol levels mirror those of brain cholesterol precursors (Fig 3b, d), though the fold-changes are less marked (figure 3f).

Brain HMG-CoA Reductase activity is decreased in YAC128 mice and increased in YAC18 mice

To further investigate the mechanism underlying defects in the cholesterol biosynthetic pathway in the presence of exogenous full-length normal and mutant huntingtin, we processed tissues for the measurement of the activity of the rate-limiting enzyme of this pathway, HMGCoAR. Purified microsomes from total brain of YAC128, YAC18 and WT mice were isolated and HMGCoAR activity evaluated. As shown in Figure 4a, HMGCoAR activity was similar in the brains of YAC128 and WT mice at 2 months of age, but at 10 months its activity was significantly decreased in YAC128 compared to WT mice (~35%, $p = 0.0298$, figure 4b). This finding is consistent with the progressive decrease in total sterols observed in the YAC128 mice (see Fig. 1). Moreover, in agreement with the increased brain levels of precursors and cholesterol (see Fig. 2 and 3), YAC18 mice showed 1.7 fold increase in HMGCoAR activity compared to WT mice and 2.5 fold compared to YAC128 mutant mice at 10-month of age (figure 4b).

Huntingtin is ubiquitously expressed, in the periphery as well as most brain regions (23), and could therefore have effects on cholesterol synthesis in organs outside the CNS. We investigated the rate of HMGCoAR activity in the liver – a crucial organ for whole body cholesterol homeostasis. Figure 4c shows that the HMGCoAR activity in microsomes purified from liver of 10-month old mice are unchanged irrespective of their genotype. Total liver sterol levels were also unchanged between genotypes at ten months (Figure 4d). These results suggest that the cholesterol biosynthetic pathway, in terms of HMGCoAR activity, is not impaired in the liver of YAC128 mice or that compensatory mechanisms occur to restore a physiological activity

of the pathway.

Plasma cholesterol and intermediate levels mirror brain sterol levels in YAC mice

Although the rate of hepatic cholesterol biosynthesis in the YAC mice was unaltered, we undertook studies to examine the plasma for alterations in cholesterol or precursor levels. Previous work has shown cholesterol biosynthetic defects in primary human fibroblasts (11), therefore alterations in cholesterol biosynthesis in cells outside the liver and brain could not be excluded and might be detected in HD plasma. In a manner analogous to the data from brain samples, no changes in plasma total cholesterol levels were found at 2 months of age (data not shown), but by 10 months of age total cholesterol levels in plasma were decreased by 13% in YAC128 compared to WT (Fig. 5a; $p<0.05$). Intriguingly, YAC18 mice showed higher plasma cholesterol level with respect to WT mice (~30%, $p = <0.001$), as well as YAC128 mice (~41%, $p < 0.001$). Next, we evaluated levels of some critical cholesterol precursors in plasma from all genotypes. We found that lanosterol (figure 5b), lathosterol (figure 5c) and desmosterol (figure 5d) were decreased in YAC128 compared to control mice, though significance was only reached for lathosterol ($p<0.05$) and desmosterol ($p<0.01$). Moreover, in agreement with the increased total cholesterol, YAC18 mice had a significant increase in plasma levels of all precursors compared to WT to YAC128 mice (Fig. 5).

These data indicate that the levels of peripheral cholesterol precursors and cholesterol itself are altered in the YAC mice with observed genotype trends paralleling those seen in the brain. This suggests that cholesterol homeostasis and/or other related-pathways outside altered in YAC mice.

Levels of 24-S-hydroxycholesterol in brain and plasma from YAC mice

Decreased levels of brain cholesterol in YAC128 mice could be entirely the consequence of the observed biosynthetic defect, or be due partly to increased catabolism. In order to investigate

whether reduced cholesterol biosynthesis in HD brain is related to an increase in cholesterol catabolism, we measured the levels of the brain-specific cholesterol metabolite 24S-hydroxycholesterol (24OHC) in the brain and plasma of YAC128, YAC18 and WT mice. As shown in figure 6, at 2 months of age, levels of 24OHC in brain were similar between YAC128 and control mice (figure 6a). However, 10-month old YAC128 mice showed a 20% and 27% reduction in the amount of brain 24OHC compared to WT ($p<0.001$) and YAC18 mice ($p<0.001$) respectively (figure 6b). The observed trend in brain 24OHC levels mirrors that observed for brain cholesterol precursors and cholesterol itself. As 24OHC, unlike cholesterol, is able to cross the blood-brain barrier (BBB) and is eliminated in the blood, we measured the levels of 24OHC in plasma. At 10 months of age 24OHC was found to be 10% and 18% lower in blood from YAC128 in comparison to WT and YAC18 mice respectively (Fig. 5c). Again, the observed trend in plasma 24OHC levels mirrors that observed for brain cholesterol biosynthesis (Fig 4b).

DISCUSSION

We have demonstrated that cholesterol homeostasis is altered in the YAC18 and YAC128 mice. Reduction in total sterol content is observed most strikingly in the striatum of the YAC128 mice, the most severely affected tissue in HD. Whole brain analysis indicates that cholesterol precursor levels are decreased as early as two months of age, before the development of neuropathology in this model. By ten months of age, a significant decrease is observable in the activity of the rate-limiting step in cholesterol biosynthesis, HMG-CoAR. Alterations of cholesterol precursors, cholesterol and 24OHC levels are also observable in the plasma of YAC mice. The YAC18 mice demonstrate a reversal of most of the cholesterol-related parameters with respect to the YAC128 phenotype, implying a role for huntingtin in cholesterol homeostasis that is modified by the presence of the mutation.

Brain cholesterol is an essential component of cellular membranes and is involved in crucial biological functions such as membrane trafficking, signal transduction, myelin formation and synaptogenesis (13). Brain cholesterol biosynthesis, storage and catabolism are in continuous balance in order to keep cholesterol levels constant and impairment in the activity of one of these elements can have a profound impact on neuronal activity and survival. According to one study, experimental reduction of cholesterol levels, or cholesterol biosynthesis, in cortical neurons is protective against NMDA induced excitotoxicity (16). This raises the intriguing possibility that the observed cholesterol reductions could be a protective response of neurons to reduce their vulnerability to excitotoxic stress. Other studies show that inhibition of HMGCoAR causes neurite loss *in vitro* (24) and mice that are unable to synthesize cholesterol in oligodendrocytes develop ataxia and tremor (25). Furthermore, a number of human diseases with neurological features are caused by abnormal brain cholesterol homeostasis including Neimann Pick type C (26) and Smith-Lemli-Opitz syndrome (27; 15).

We have previously shown that mRNA levels of key genes involved in cholesterol

biosynthesis are reduced in the brain of R6/2 transgenic mice, which express a fragment of mutant huntingtin, and in neuronal tissue from post-mortem HD patients and human HD fibroblasts (11). We have identified impaired SREBP nuclear translocation as the underlying molecular mechanism. The biological effects of altered SREBP transport are reduced total sterol production in neuronal tissues of R6/2 mice and reduced *de novo* cholesterol biosynthesis in human HD fibroblasts (11).

Here we have extended these data by showing that cholesterol dysfunction occurs in a full-length mouse model of HD, the YAC128 mouse (17). The YAC128 mice demonstrate specific neuropathology (17, 18), which closely mirrors the atrophy observed in human HD patients. Another benefit of the YAC128 in studies such as these is the longer course of disease, allowing consideration of the sequence, timing and natural history of pathological events.

An interesting finding of this study is that YAC18 mice over-expressing normal huntingtin show differences in most cholesterol related phenotypes compared to WT and YAC128 mice. This suggests that the cholesterol alterations observed are not a secondary consequence of mice displaying HD phenotypes, but rather that the huntingtin protein itself may play a key role in cholesterol homeostasis.

The tissue-specific neuropathology of the YAC128 mice lends interest to our finding that total sterols are reduced in the striatum of 10-month old YAC128 mice with respect to controls. Tissues relatively spared in HD, as well as in the YAC128 model, such as the cerebellum (18) maintain normal sterol levels, reinforcing the coincident nature of sterol loss and neuronal atrophy. Different neuronal populations and brain areas require different amounts of sterols, leaving them more or less vulnerable to cholesterol deficiency (28). Due to its unique anatomical/functional demands, cholesterol levels in the striatum are approximately 1.5 fold higher than the cortex (29, 30). We confirmed this in our experiments by showing that total sterols in control striata reached values of 25 μg/mg while only 12.5 μg/mg can be measured in cortical tissues. The evidence that the striatum of YAC128 mice showed a 40% reduction in sterol levels, whereas cortical losses

were milder, suggests that a cholesterol dysfunction might contribute to the tissue-specific vulnerability of brain regions observed in HD (15).

The YAC128 mice have allowed us to demonstrate that brain and plasma levels of cholesterol are unaltered at 2 months of age, suggesting that cholesterol biosynthesis during development is unaffected in these mice. This implies that either the cholesterol biosynthetic role of huntingtin is not important during development, or that it is able to fulfill this role for a time. In the adult brain cholesterol biosynthesis decreases to stable levels, occurring in neurons and astrocytes, with astrocytes producing approximately three fold more cholesterol than neurons (31, 32). Mutant huntingtin may interfere with this *de novo* cholesterol production (estimated 1-2 mg/day in humans; 33) that, while small, is crucial for neuronal survival and maintenance.

Lanosterol and lathosterol levels are considered to be indicators of cholesterol *neo*-genesis, and are decreased by 2 months of age in the brain of YAC128 mice, before changes in cholesterol accumulation are observed. During later points the lathosterol deficits become more pronounced, while the cholesterol levels are also affected. This suggests a model in which cholesterol biosynthetic defects are seen early, preceding overt neuropathology, with detectable decreases in cholesterol accumulation developing in parallel with the brain atrophy. The difference in magnitude between precursor and cholesterol reduction may be due to the fact that the cholesterol levels measured include the cholesterol in myelin sheaths, which makes up the bulk of brain cholesterol (34). This store of cholesterol seems not affected by the huntingtin mutation, because YAC128 mice demonstrate normal brain cholesterol levels at 2-month of age. Moreover, brain cholesterol has a half-life that is at least 100 times longer than that of cholesterol in most other organs. The half life of the total bulk of brain cholesterol is estimated to be 4-6 months in mice and rats (35) and 5 years in humans (36), suggesting that significant developmental sources of cholesterol may persist in YAC128 brains to the 10-month time point analyzed here.

Analyzing different components of the cholesterol biosynthesis cascade – lanosterol, desmosterol and lathosterol – did not reveal any accumulation of intermediates in YAC128 brains

suggesting that no specific inhibitions occur in crucial steps of the pathway. Evidence of altered activity of HMGCoAR, the upstream rate-limiting enzyme that catalyzes the formation of mevalonate, in YAC mouse brain indicates that the biosynthetic pathway is affected from its first steps. This is consistent with our earlier work demonstrating impaired nuclear translocation of SREBPs in HD tissues (11).

Several intermediate products produced from mevalonate have independent functions (37; see also Fig. 2a). For instance, isoprenoids including farnesyl and geranylgeranyl diphosphates are important components of molecules including GTP binding proteins. These proteins play diverse roles within cells ranging from intracellular signaling to vesicular transport (38). Other molecules, such as hemeA and ubiquinone (coenzyme Q10), which take part in electron transport, and dolichol, required for glycoprotein synthesis, are synthesized from the intermediary metabolites of the cholesterol biosynthetic pathway. Therefore, a defect at multiple steps of this pathway may lead not only to decreased levels of newly cholesterol but also to reduced supply of intermediate products affecting important metabolic functions within the HD cells.

We have shown reductions in plasma levels of cholesterol and cholesterol precursors in YAC128 mice when compared to WT and YAC18 mice, with observed trends closely paralleling levels in brain in the same mice. Plasma cholesterol alterations were not due to altered hepatic biosynthesis, as demonstrated by unaffected HMG-CoAR activity and total sterol levels in the liver. In addition to the liver, the intestine has been shown to contribute approximately 30% of plasma HDL cholesterol in mice (39), therefore it is possible that the reduction in plasma cholesterol observed in the YAC128 mice could be explained by decreased cholesterol biosynthesis outside the liver or brain.

The majority of plasma 24OHC is brain-derived, allowing its levels in blood to be taken as an index of brain cholesterol elimination (20). We report that at 10 months of age there is a significant reduction of 24OHC levels in brain and plasma from YAC128 mice that correlates with

brain cholesterol biosynthetic defects. When levels of 24OHC are considered as a ratio to total brain cholesterol, no differences are observed in any of the genotypes tested – suggesting that the rate of flux through the 24OHC pathway is unaltered. This, in conjunction with the observed correlation between brain and plasma 24OHC levels observed in all genotypes highlights the fact that 24OHC in plasma reflects brain cholesterol biosynthesis. The evidence that brains of 2-month old YAC128 mice have reduced levels of lanosterol and lathosterol but not of 24OHC implies that the biosynthetic defect occurs initially, followed by a progressive decrease in total cholesterol, followed by decreased production of 24OHC due to reduced substrate concentrations.

In conclusion, our findings demonstrate that cholesterol homeostasis alterations occur in the YAC128 mice. We show that in YAC128 this dysfunction is most pronounced in the striatum, appears early and is progressive. Moreover, our data suggest that normal huntingtin may play an important role in cholesterol biosynthesis.

MATERIALS AND METHODS

Mice and tissues Experiments were carried out on YAC18 and YAC128 mice generated to express wild-type huntingtin with 18 glutamines (19) and mutant huntingtin with 120 glutamines, respectively (17) and littermate (WT) mice. YAC18 mice express exogenous wild type human huntingtin under the same regulatory control as the YAC128 mice. Expression levels of transgenic huntingtin in the YAC128 (line 53) and YAC18 (line 212) lines used in the current study are equivalent. After overnight starvation, the animals were sacrificed at different disease stages and perfused with saline, after which their brains were isolated or dissected in order to separate the different neuronal areas. The animals were cared for in accordance with our institutional guidelines.

Enzymatic measurement of total sterols. In order to measure total sterol levels enzymatically, neuronal and hepatic tissues were homogenated and lipid fraction was isolated by means of solvent extraction (chloroform: methanol 3:2 (v/v) in presence of butylated hydroxytoluene (BHT) 25ug/ml). Total sterol content was then assayed using the Cholesterol kit (FAR srl, Italy) as instructed by the manufacturer. The amounts of sterol were normalised on the basis of wet tissue weight.

Isotopic dilution mass spectrometry measurements of neutral sterols and oxysterols. Tissue homogenates were prepared in PBS containing 0.25 M sucrose (10% w/v); 30µL of homogenated tissues were added to a screw-capped vial sealed with a Teflon-lined septum, together with 100 ng of 5a-cholest-7-en-3b-ol-1,2,5a,6a-d4 (2H4-lathosterol, CDN Isotopes), 200 ng of [2H3]24S-hydroxycholesterol, and 200 ng of [2H6] 27-hydroxycholesterol (50 µL from a methanolic solution of 4 mg/L of each of the deuterated-oxysterols) as internal standards. To prevent self-oxidation, 25 µL of butylated hydroxytoluene (BHT) (5 g/L) and 25 µL of EDTA (10 g/L) were added to each

vial, and argon was flushed through in order to remove air. Alkaline hydrolysis was allowed to proceed at room temperature (22°C) for one hour in the presence of 1 M ethanolic potassium hydroxide solution under magnetic stirring. After hydrolysis, the neutral sterols (cholesterol, lathosterol, desmosterol and lanosterol) and oxysterol (24-OHC) were extracted three times with 5 mL of cyclohexane. The organic solvents were evaporated under a gentle stream of argon, and converted into trimethylsilyl ethers (pyridine:hexamethyldisilazane:trimethylchlorosilane, 3:2:1 (v/v/v)).

Gas chromatography-mass spectrometry (GC-MS) was performed on an Agilent Technologies HP 5890 series II combined with a 5972 mass selective detector. The GC was equipped with a DB-XLB (30 m x 0.25 mm id x 0.25 µm film; J&W, Palo Alto, CA, USA), and the injection was made in the splitless mode using helium (1 mL/min) as a carrier gas. The initial temperature of 150°C was maintained for one minute, increased by 20°C/min up to 260°C, and then by 10°C/minute up to the end- temperature of 280°C, which was maintained for 15 minutes. The mass spectrometer was used in selected ion-monitoring mode, and the neutral sterols were monitored as their TMSi derivates using the following masses: 2H4-lathosterol at 462 m/z (M+-OTMSi), lathosterol at 458 m/z (M+-OTMSi), desmosterol at m/z 441 (M+-OTMSi), lanosterol at 498 m/z (M+-OTMSi), 24OHC at 413 m/z (M+-OTMSi), and [2H3]24-OHC at 416 m/z (M+-OTMSi). Peak integration was performed manually, and the sterols were quantified from the selected-ion monitoring analyses against internal standards using standard curves. The identity of all of the sterols was proven by comparison with the full-scan mass spectra of authentic compounds. Additional qualifier ions (characteristic fragment ions) were used for structural identification.

Preparation of microsomes and assay of HMG-CoA reductase activity. The brain and liver homogenates were prepared in PBS containing 0.25 M sucrose (10% w/v), and an aliquot was used to measure the sterols and oxysterols by means of isotopic-dilution mass spectrometry. The

microsomal fractions were isolated as previously described (40) and then resuspended in 50 mM phosphate buffer, pH 7.4, containing 5mM DTT, 200mM KCl, 1mM EDTA, and 0.25% Brij96. The protein concentrations of the microsomal fractions were determined using Lowry's method. HMGCoA reductase was assayed essentially as described by Brown, Goldstein and Dietschy (41) with some modifications: 0.04 μCi of [3-^{14C}]HMG-CoA (specific activity 54.6 mCi/mmol) were preincubated in 0.3 ml of buffer containing 200 mM phosphate buffer, pH 7.4, 8.3 mM DTT (Sigma), 4mM NADPH (Sigma) and 40 mM glucose-6-phosphate (Sigma) for 10 min at 37°C, after which 100 μg of microsomal proteins were added, and the HMG-CoA reductase assay was run for 2 h at 37°C. The assay was stopped by the addition of 20 μl of STOP solution containing 5N HCl, 7 μCi tritium-labelled mevalonic acid (33.00 Ci/mmol) and unlabelled mevalonic acid lactone. The enzyme assays were carried out in triplicate in all of the experiments. After lactonisation, the incubation mixture underwent thin-layer chromatography, with benzene-acetone 1:1 (v/v) being used as the developing solvent. The mevalonic acid lactone zone was located and scraped off into a counting vial, and a Packard liquid scintillation spectrometer (Tri-Carb 2100TR, Packard) was used to determine radioactivity with Insta-Gel Plus (Perkin-Elmer) as scintillator liquid. Corrections for losses were made using the internal standard.

Plasma cholesterol and precursors levels by gas chromatography and GS-MS

To analyse plasma samples 50 μg 5a-cholestane (Serva, Feinbiochemica GmbH, Heidelberg, Germany) (50 μL from a stock solution of 5a-cholestane in cyclohexane; mg/mL), 1 μg epicoprostanol (Sigma, Seelze, Germany) (10 μL from a stock solution epicoprostanol in cyclohexane; 100 μg/mL) and 100 ng [23,23,24,25-2H4]24R,S-hydroxycholesterol (50 μL from a stock solution of [2H4]24R,S-hydroxycholesterol in methanol; 2 mg/mL), as internal standards, respectively, were added two 100 μl plasma. Solvolysis, extraction and derivatization were performed as described previously (42). The residue was dissolved in 60 μL n-decane. Fifty μl of

the solution was transferred into a micro-vial for gas-liquid chromatography-mass spectrometry-selected ion monitoring (GC-MS-SIM) analysis of cholesterol precursors, lathosterol, lanosterol, and desmosterol and the cholesterol metabolite 24S-hydroxycholesterol. Ten µL was diluted with 90 µL n-decane for analysis of cholesterol by gas-liquid chromatography-flame ionization detection (GC-FID) (43). The variability of within-day and between-day accuracy and precision for all analytes was lower than 4% of the respective nominal and mean values, respectively. Identity of all sterols was proven by comparison with the full scan mass spectra of authentic compounds.

Statistical analysis. The data were compared using different statistical approaches such as t-test analysis, One-way ANOVA with Newman-Keuls Multiple comparison Test or Mann-Whitney Test, as indicated. P-values, SEM, SD and means were calculated using Graphpad Prism version 4.0.

ACKNOWLEDGEMENTS

We are grateful to S. Fenu, J. Karaskinska and M. Pouladi for their helpful comments and suggestions and to L. Petricca for her precious technical support. This work was supported by Telethon (#112, Italy) and NeuroNE (FP6, EU) to EC; Ministero della Salute (Ex art. 56, Italy) to SdD; Fondazione Cariplo (Prot. 2003-1602, Italy) to EC and SdD; the Canadian Institutes of Health Research, the Huntington Society of Canada, the Hereditary Disease Foundation and the Canadian Genetic Diseases Network to MRH; the Swedish Science Council (Sweden) and the Foundation BLANCEFLOR Boncompagni-Ludovisi, n`ee Bildt and Brain Power (Sweden) to IB and VL. MV is supported by *Sovvenzione Globale INGENIO* (European Social Found, 2006) and JBC is supported by the Huntington Society of Canada. MRH is a Killam University Professor and holds a Canada Research Chair in Human Genetics.

REFERENCES

1. (1993) A novel gene containing a trinucleotide repeat that is expanded and unstable on Huntington's disease chromosomes. The Huntington's Disease Collaborative Research Group. *Cell*, **72**, 971-983.

2. Nasir, J., Floresco, S.B., O'Kusky, J.R., Diewert, V.M., Richman, J.M., Zeisler, J., Borowski, A., Marth, J.D., Phillips, A.G. and Hayden, M.R. (1995) Targeted disruption of the Huntington's disease gene results in embryonic lethality and behavioral and morphological changes in heterozygotes. *Cell*, **81**, 811-823.

3. Duyao, M.P., Auerbach, A.B., Ryan, A., Persichetti, F., Barnes, G.T., McNeil, S.M., Ge, P., Vonsattel, J.P., Gusella, J.F., Joyner, A.L. et al. (1995) Inactivation of the mouse Huntington's disease gene homolog Hdh. *Science*, **269**, 407-410.

4. Zeitlin, S., Liu, J.P., Chapman, D.L., Papaioannou, V.E. and Efstratiadis, A. (1995) Increased apoptosis and early embryonic lethality in mice nullizygous for the Huntington's disease gene homologue. *Nat. Genet.*, **11**, 155-163.

5. Cattaneo, E., Zuccato, C. and Tartari, M. (2005) Normal huntingtin function: an alternative approach to Huntington's disease. *Nat. Rev. Neurosci.*, **6**, 919-930.

6. DiFiglia, M., Sapp, E., Chase, K.O., Davies, S.W., Bates, G.P., Vonsattel, J.P. and Aronin, N. (1997) Aggregation of huntingtin in neuronal intranuclear inclusions and dystrophic neurites in brain. *Science*, **277**, 1990-1993.

7. Vonsattel, J.P., Myers, R.H., Stevens, T.J., Ferrante, R.J., Bird, E.D. and Richardson, E.P., Jr. (1985) Neuropathological classification of Huntington's disease. *J. Neuropathol. Exp. Neurol.*, **44**, 559-577.

8. Vonsattel, J.P. and DiFiglia, M. (1998) Huntington disease. *J. Neuropathol. Exp. Neurol.*, **57**,

369-384.

9. Sipione, S., Rigamonti, D., Valenza, M., Zuccato, C., Conti, L., Pritchard, J., Kooperberg, C., Olson, J.M. and Cattaneo, E. (2002) Early transcriptional profiles in huntingtin-inducible striatal cells by microarray analyses. *Hum. Mol. Genet*., **11**, 1953-1965.

10. Mangiarini, L., Sathasivam, K., Seller, M., Cozens, B., Harper, A., Hetherington, C., Lawton, M., Trottier, Y., Lehrach, H., Davies, S.W. et al. (1996) Exon 1 of the HD gene with an expanded CAG repeat is sufficient to cause a progressive neurological phenotype in transgenic mice. *Cell*, **87**, 493-506.

11. Valenza, M., Rigamonti, D., Goffredo, D., Zuccato, C., Fenu, S., Jamot, L., Strand, A., Tarditi, A., Woodman, B., Racchi, M. et al. (2005) Dysfunction of the cholesterol biosynthetic pathway in Huntington's disease. *J. Neurosci*., **25**, 9932-9939.

12. Jurevics, H. and Morell, P. (1995) Cholesterol for synthesis of myelin is made locally, not imported into brain. *J. Neurochem*., **64**, 895-901.

13. Dietschy, J.M. and Turley, S.D. (2004) Thematic review series: brain Lipids. Cholesterol metabolism in the central nervous system during early development and in the mature animal. *J. Lipid. Res.*, **45**, 1375-1397.

14. Mauch, D.H., Nagler, K., Schumacher, S., Goritz, C., Muller, E.C., Otto, A. and Pfrieger, F.W. (2001) CNS synaptogenesis promoted by glia-derived cholesterol. *Science*, **294**, 1354-1357.

15. Valenza, M. and Cattaneo, E. (2006) Cholesterol dysfunction in neurodegenerative diseases: is Huntington's disease in the list? *Prog. Neurobiol*., **80**, 165-176.

16. Zacco, A., Togo, J., Spence, K., Ellis, A., Lloyd, D., Furlong, S. and Piser, T. (2003) 3-hydroxy-3-methylglutaryl coenzyme A reductase inhibitors protect cortical neurons from excitotoxicity. *J. Neurosci*., **23**, 11104-11111.

17. Slow, E.J., van Raamsdonk, J., Rogers, D., Coleman, S.H., Graham, R.K., Deng, Y., Oh, R.,

Bissada, N., Hossain, S.M., Yang, Y.Z. et al. (2003) Selective striatal neuronal loss in a YAC128 mouse model of Huntington disease. *Hum. Mol. Genet.*, **12**, 1555-1567.

18. Van Raamsdonk, J.M., Murphy, Z., Slow, E.J., Leavitt, B.R. and Hayden, M.R. (2005) Selective degeneration and nuclear localization of mutant huntingtin in the YAC128 mouse model of Huntington disease. *Hum. Mol. Genet.*, **14**, 3823-3835.

19. Hodgson, J.G., Agopyan, N., Gutekunst, C.A., Leavitt, B.R., LePiane, F., Singaraja, R., Smith, D.J., Bissada, N., McCutcheon, K., Nasir, J. et al. (1999) A YAC mouse model for Huntington's disease with full-length mutant huntingtin, cytoplasmic toxicity, and selective striatal neurodegeneration. *Neuron*, **23**, 181-192.

20. Lund, E.G., Xie, C., Kotti, T., Turley, S.D., Dietschy, J.M. and Russell, D.W. (2003) Knockout of the cholesterol 24-hydroxylase gene in mice reveals a brain-specific mechanism of cholesterol turnover. *J. Biol. Chem.*, **278**, 22980-22988.

21. Jira, P.E., de Jong, J.G., Janssen-Zijlstra, F.S., Wendel, U. and Wevers, R.A. (1997) Pitfalls in measuring plasma cholesterol in the Smith-Lemli-Opitz syndrome. *Clin. Chem.*, **43**, 129-33.

22. Kempen, H.J., Glatz, J.F., Gevers Leuven, J.A., van der Voort, H.A. and Katan, M.B. (1988) Serum lathosterol concentration is an indicator of whole-body cholesterol synthesis in humans. *J. Lipid. Res.*, **29**, 1149-1155.

23. Trottier, Y., Devys, D., Imbert, G., Saudou, F., An, I., Lutz, Y., Weber, C., Agid, Y., Hirsch, E.C. and Mandel, J.L. (1995) Cellular localization of the Huntington's disease protein and discrimination of the normal and mutated form. *Nat. Genet.*, **10**, 104-110.

24. Schulz, J.G., Bosel, J., Stoeckel, M., Megow, D., Dirnagl, U. and Endres, M. (2004) HMG-CoA reductase inhibition causes neurite loss by interfering with geranylgeranylpyrophosphate synthesis. *J. Neurochem.*, **89**, 24-32.

25. Saher, G., Brugger, B., Lappe-Siefke, C., Mobius, W., Tozawa, R., Wehr, M.C., Wieland, F., Ishibashi, S. and Nave, K.A. (2005) High cholesterol level is essential for myelin membrane

growth. *Nat. Neurosci*., **8**, 468-475.

26. Crocker, A.C. (1961) The cerebral defect in Tay-Sachs disease and Niemann-Pick disease. *J. Neurochem*., **7**, 69-80.

27. Tint, G.S., Irons, M., Elias, E.R., Batta, A.K., Frieden, R., Chen, T.S. and Salen, G. (1994) Defective cholesterol biosynthesis associated with the Smith-Lemli-Opitz syndrome. *N. Engl. J. Med*., **330**, 107-113.

28. Pfrieger, F.W. (2003) Cholesterol homeostasis and function in neurons of the central nervous system. *Cell. Mol. Life Sci*., **60**, 1158-1171.

29. Zhang, Y., Appelkvist, E.L., Kristensson, K. and Dallner, G. (1996) The lipid compositions of different regions of rat brain during development and aging. *Neurobiol. Aging*, **17**, 869-875.

30. Runquist, M., Parmryd, I., Thelin, A., Chojnacki, T. and Dallner, G. (1995) Distribution of branch point prenyltransferases in regions of bovine brain. *J. Neurochem*., **65**, 2299-2306.

31. Saito, M., Benson, E.P., Saito, M. and Rosenberg, A. (1987) Metabolism of cholesterol and triacylglycerol in cultured chick neuronal cells, glial cells, and fibroblasts: accumulation of esterified cholesterol in serum-free culture. *J. Neurosci. Res*., **18**, 319-325.

32. Bjorkhem, I. and Meaney, S. (2004) Brain cholesterol: long secret life behind a barrier. *Arterioscler. Thromb. Vasc. Biol*., **24**, 806-815.

33. Lutjohann, D., Breuer, O., Ahlborg, G., Nennesmo, I., Siden, A., Diczfalusy, U. and Bjorkhem, I. (1996) Cholesterol homeostasis in human brain: evidence for an age-dependent flux of 24S-hydroxycholesterol from the brain into the circulation. *Proc. Natl. Acad. Sci. U S A*, **93**, 9799-9804.

34. Snipes, G.J. and Suter, U. (1997) Cholesterol and myelin. *Subcell. Biochem*., **28**, 173-204.

35. Andersson, M., Elmberger, P.G., Edlund, C., Kristensson, K. and Dallner, G. (1990) Rates of cholesterol, ubiquinone, dolichol and dolichyl-P biosynthesis in rat brain slices. *FEBS Lett*., **269**,

15-18.

36. Bjorkhem, I., Lutjohann, D., Diczfalusy, U., Stahle, L., Ahlborg, G. and Wahren, J. (1998) Cholesterol homeostasis in human brain: turnover of 24S-hydroxycholesterol and evidence for a cerebral origin of most of this oxysterol in the circulation. *J. Lipid. Res*., **39**, 1594-1600.

37. Horton, J.D., Goldstein, J.L. and Brown, M.S. (2002) SREBPs: activators of the complete program of cholesterol and fatty acid synthesis in the liver. *J. Clin. Invest*., **109**, 1125-1131.

38. Pfeffer, S. and Aivazian, D. (2004) Targeting Rab GTPases to distinct membrane compartments. *Nat. Rev. Mol. Cell. Biol*., **5**, 886-896.

39. Brunham, L.R., Kruit, J.K., Iqbal, J., Fievet, C., Timmins, J.M., Pape, T.D., Coburn, B.A., Bissada, N., Staels, B., Groen, A.K. et al. (2006) Intestinal ABCA1 directly contributes to HDL biogenesis in vivo. *J. Clin. Invest*., **116**, 1052-1062.

40. Angelin, B., Einarsson, K., Liljeqvist, L., Nilsell, K. and Heller, R.A. (1984) 3-hydroxy-3-methylglutaryl coenzyme A reductase in human liver microsomes: active and inactive forms and cross-reactivity with antibody against rat liver enzyme. *J. Lipid. Res*., **25**, 1159-1166.

41. Brown, M.S., Goldstein, J.L. and Dietschy, J.M. (1979) Active and inactive forms of 3-hydroxy-3-methylglutaryl coenzyme A reductase in the liver of the rat. Comparison with the rate of cholesterol synthesis in different physiological states. *J. Biol. Chem*., **254**, 5144-5149.

42. Lutjohann, D., Brzezinka, A., Barth, E., Abramowski, D., Staufenbiel, M., von Bergmann, K., Beyreuther, K., Multhaup, G. and Bayer, T.A. (2002) Profile of cholesterol-related sterols in aged amyloid precursor protein transgenic mouse brain. *J. Lipid. Res*., **43**, 1078-1085.

43. Locatelli, S., Lutjohann, D., Schmidt, H.H., Otto, C., Beisiegel, U. and von Bergmann, K. (2002) Reduction of plasma 24S-hydroxycholesterol (cerebrosterol) levels using high-dosage simvastatin in patients with hypercholesterolemia: evidence that simvastatin affects cholesterol metabolism in the human brain. *Arch. Neurol*., **59**, 213-216.

LEGENDS TO FIGURES

Figure 1. Total sterol levels are specifically reduced in the striatum from 10 months old YAC128 mice. (a) Striatal total sterol levels were significantly reduced in YAC128 compared to WT ($P<0.001$) and YAC18 mice ($P<0.001$). (b) Cortical total sterol levels of YAC128 mice were not found significantly different with respect to WT mice. Slight cortical sterol reduction was found in YAC128 vs YAC18 mice, using a non-parametric analysis ($^{\#}p=0.048$; Mann Whitney Test). (c) Cerebellar total sterols were not found to be different in the three genotypes. Total sterols were evaluated by means of enzymatic method as described in material and methods. The sterol values are expressed as µg above mg tissue and are the average of three (YAC128; YAC18) or six (WT) independent mice from each genotype; each sample was analyzed in triplicate and the graphs represent one of the three experiments performed. Error bars show standard error of the mean (SEM). Statistics, One-way ANOVA, Newman-Keuls Multiple Comparison Test. Significant differences are represented by asterisks. ***$P<0.001$.

Figure 2. Levels of brain lathosterol, indicator of cholesterol neo-genesis, are progressively reduced in YAC128 mice but are increased in YAC18 mice. (a) Simplified view of cholesterol biosynthetic pathway. Lanosterol, lathosterol, desmosterol (in bold) are the principal precursors of the cholesterol biosynthetic pathway. The HmgCoAR (in bold) is the rate-limiting enzyme of the pathway. (b) Lathosterol levels were significantly decreased in YAC128 mice compared to WT mice at 2 months of age, before neuropathology occurred ($p=0.0298$). (c) Lathosterol levels were significantly decreased in 10-month old YAC128 mice compared to WT and more to YAC18 mice (p value summary < 0.0001). 10-month old YAC18 mice showed significant higher levels of lathosterol compared to WT mice ($p<0.01$) and to YAC128 mice ($p<0.001$). Lathosterol was measured by means of isotopic-dilution mass spectrometry. The values are expressed above wet weight of tissue (ww) and are the average of four (YAC128) and four (WT) independent mice at 2

months of age and three (YAC128), four (WT) and three (YAC18) independent mice at 10 months of age. Each sample was analyzed in triplicate. Error bars show SEM. Statistics, unpaired t-test and One-way ANOVA, Newman-Keuls Multiple Comparison Test. Significant differences are represented by asterisks. *P<0.05; **P<0.01; ***P<0.001.

Figure 3. Levels of other key-cholesterol precursors, lanosterol and desmosterol, are progressively reduced in brain of YAC128 mice leading to reduced total cholesterol account at later stages. YAC18 mice show higher levels of biosynthetic components of the pathway as well as total cholesterol with respect to WT and more to YAC128 mice. (a, b) Lanosterol levels were significantly reduced in YAC128 mice since 2 months of age (p= 0.02) and persist at 10 months of age (p< 0.05). Desmosterol levels were similar at 2 months of age between mutant and littermate mice but were significantly increased in 10-month old YAC128 mice compared to WT and YAC128 mice (p value summary = 0.0276). (c) Cholesterol amount was found similar at 2 months of age between YAC128 and WT mice. (d) Cholesterol was slightly decreased, with the same pattern, in YAC128 mice compared to WT and YAC18 mice (p value summary = 0.0315). YAC128 mice showed higher levels of lanosterol (b), desmosterol (d) and total cholesterol (f) with respect to WT and more to YAC128 mice, although the significance has been reached only vs YAC128 (P < 0.05). Sterols were measured by means of isotopic-dilution mass spectrometry. The values are the average of independent mice from each genotype and each sample was analyzed in triplicate. N = 4 YAC128, 4 WT at 2 months of age. N = 4 YAC128, 4 WT and 3 YAC18 mice at 10 months of age. Error bars show SEM. Statistics, unpaired t-test and One-way ANOVA, Newman-Keuls Multiple Comparison Test. Significant differences are represented by asterisks or P value given. *P<0.05; **P<0.01; ***P<0.001.

Figure 4. Microsomal HMGCoAR activity is specifically reduced in brain of 10-month old

YAC128 and significantly increased in YAC18 mice. (a) HMGCoAR activity is unchanged at pre-neuropathology stage (2 months of age) in brain from YAC128 with respect to WT mice. (b) HMGCoAR activity was significantly reduced in brain of 10-month old YAC128 mice compared to WT ($p<0.01$) and YAC18 mice ($p<0.01$). Siginficant difference was also found between WT and YAC18 ($p<0.01$). (c) Microsomal HMGCoAR activity (c) and total sterols as measured by enzymatic method (d) were not found different in the three genotypes at 10 months of age. The values are the average of three (YAC128), four (WT) and three (YAC18) independent mice analyzed in triplicate. The data are expressed as percentages above WT values. Error bars show standard deviations (SD). Statistics, One-way ANOVA, Newman-Keuls Multiple Comparison Test. Significant differences are represented by asterisks. **P<0.01.

Figure 5. Levels of plasma cholesterol are reduced in the YAC128 mice and increased in YAC18 mice at 10 months of age. (a) Total cholesterol, as determined by GC-MS, is significantly reduced in the plasma of 10 month old YAC128 mice ($p < 0.05$), while it is increased in the YAC18 mice relative to WT controls ($p < 0.001$) and YAC128's ($p < 0.001$). (b-d) Levels of the cholesterol precursors lanosterol, lathosterol and desmosterol in the plasma of 10-month old animals show the same trends as plasma cholesterol – decreased in the YAC128 and increased in the YAC18 relative to WT controls. (b) Trend reduction in lanosterol levels was observed in YAC128 when compared to WT and YAC18 mice, despite significances were not reached ($p > 0.05$). (c) Differences in lathosterol levels were found to be significant for YAC128 vs. WT ($p < 0.05$) as well as YAC128 vs. YAC18 ($p < 0.01$). (d) Significant differences were also found in desmosterol levels in YAC128 in comparison to WT ($p < 0.01$) and YAC18's ($p < 0.001$). The YAC18 levels of desmosterol were also found to be significantly increased compared to WT mice ($p < 0.01$). All the plasma values are the average of 10 (YAC128), 13 (WT) and 7 (YAC18) independent mice from each genotype and are normalized above respective WT values. Error bars show SEM. Statistics, One-way ANOVA, Newman-Keuls Multiple Comparison Test. Significant differences are

represented by asterisks.*P < 0.05; **P < 0.01; ***P < 0.001.

Figure 6. Brain and plasma levels of 24OHC, a brain-specific cholesterol catabolite, are progressively reduced in YAC128 mice and increased in YAC18 mice. (a) At 2 months of age, the brain levels of 24OHC were found similar in YAC128 and WT mice. (b) At 10 months of age, levels of 24OHC were significantly reduced in brain from YAC128 mice compared to WT mice and to YAC18 mice (p value summary = 0.0002). (c) Plasma levels of 24OHC were found reduced in same matched-aged YAC128 with respect to WT and YAC18 mice (p value summary = 0.0061). Brain and plasma 24OHC was measured by means of isotopic dilution mass spectrometry. The brain values are the average of independent mice and each sample was analyzed in triplicate. N = 4 YAC128, 4 WT at 2 months of age; N = 4 YAC128, 4 WT and 3 YAC18 mice at 10 months of age. Plasma values are the average of 10 (YAC128), 13 (WT) and 7 (YAC18) independent mice from each genotype and are normalized above WT values. Error bars show SEM. Statistics, One-way ANOVA, Newman-Keuls Multiple Comparison Test. Significant differences are represented by asterisks.*P < 0.05; **P < 0.01; ***P < 0.001.

Table 1. Reduction of striatal and cortical sterol accumulation in YAC128 mice from 2 to 18 months of age. The values represent the average of three YAC128 and WT independent mice from each genotype; For each tissue (striatum or cortex), the data are expressed as percentage above mean of total sterols (µg/mg tissue) of 2-month old for each genotype. Statistics, t test analysis. YAC128 striatum (18ms) *vs* WT striatum (18ms), ***P<0.001; YAC128 cortex (18ms) *vs* WT cortex (18 ms), $^{\S}p = 0.068$.

Table 1. Reduced sterol accumulation in striatum and cortex over time in YAC128 mice.

	Striatum (% μg/mg tissue)	
	2 months	18 months
WT	100.0 ± 3.96	145.2 ± 0.72
YAC128	100.0 ± 4.51	110.3 ± 2.80***
	Cortex (% μ g/mg tissue)	
	2 months	18 months
WT	100.0 ± 3.50	126.0 ± 5.64
YAC128	100.0 ± 6.04	114.1 ± 3.63§

Table 1

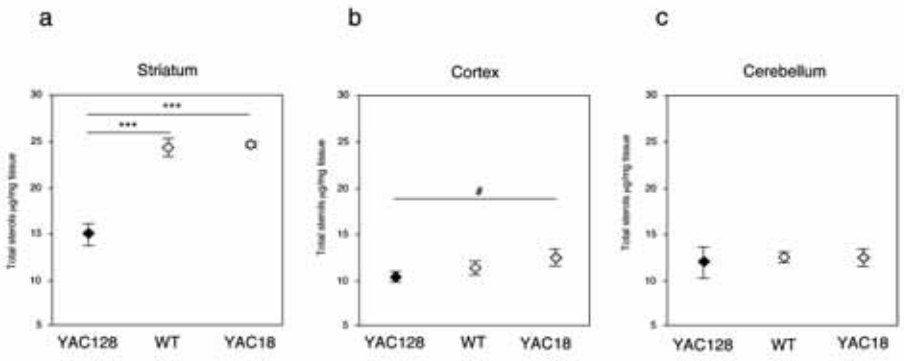

Figure 1

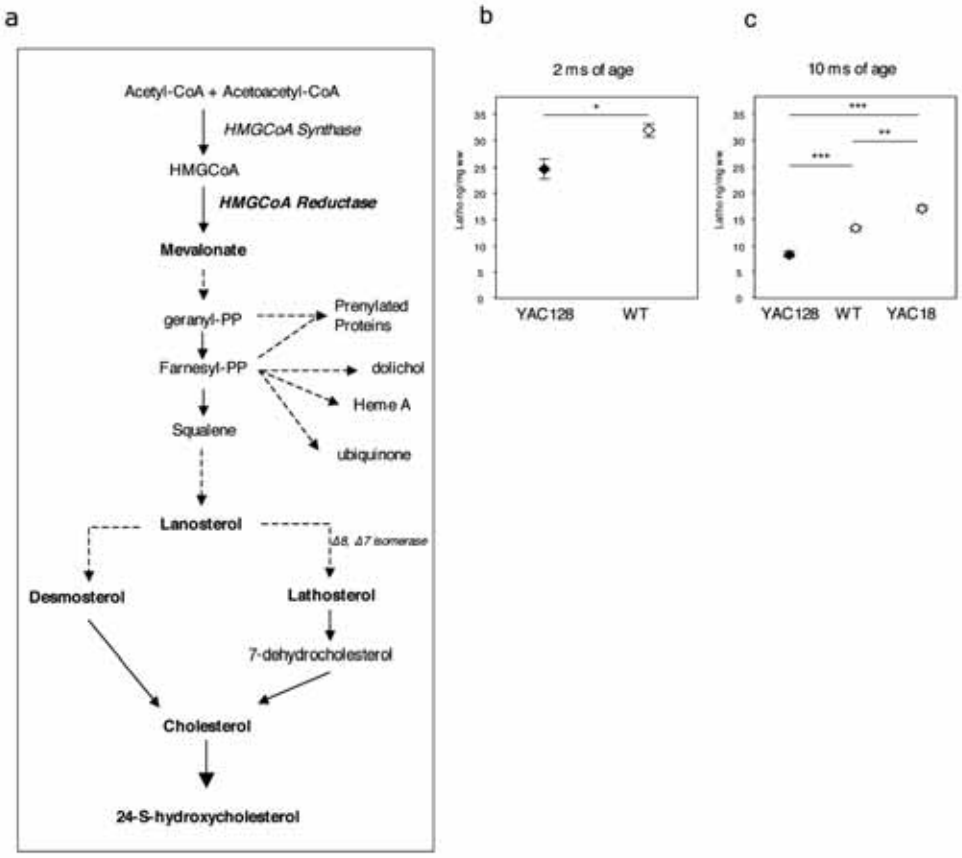

Figure 2

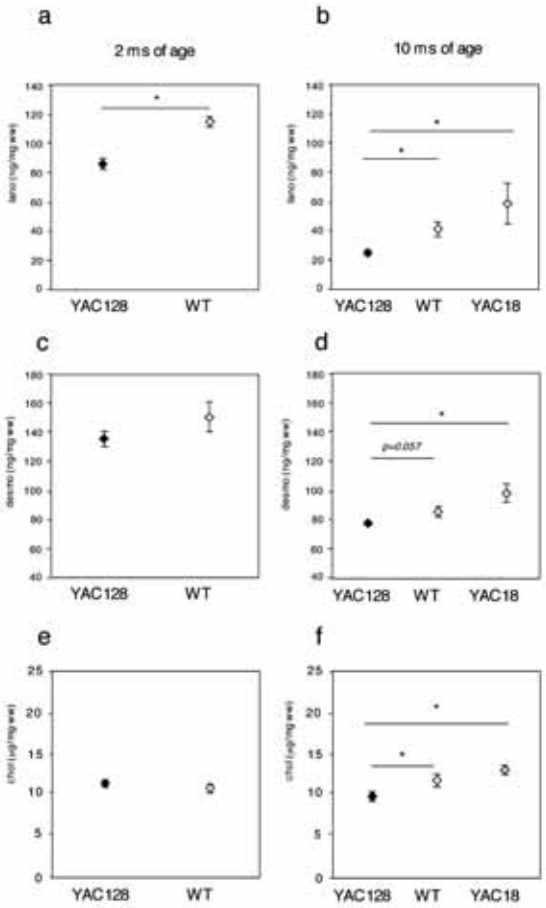

Figure 3

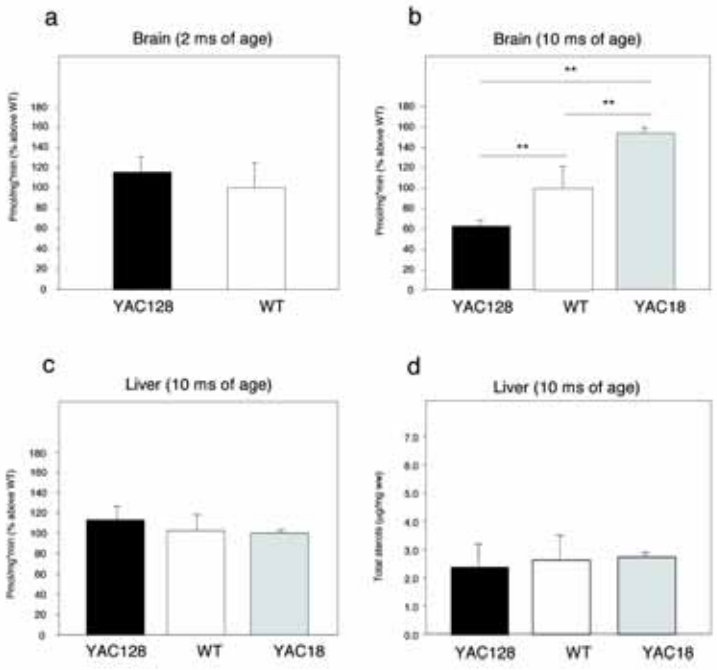

Figure 4

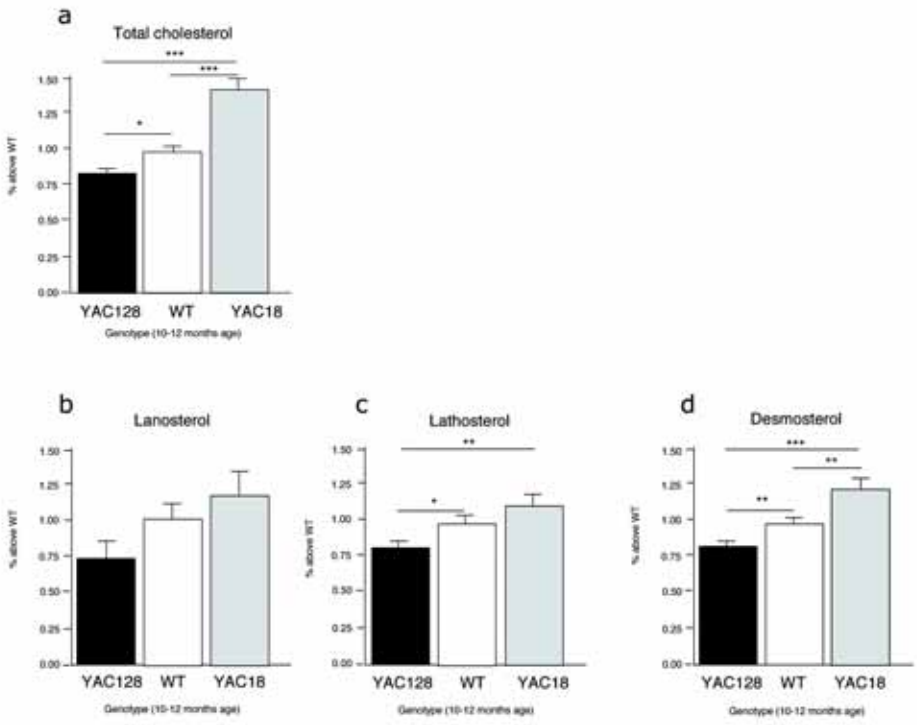

Figure 5

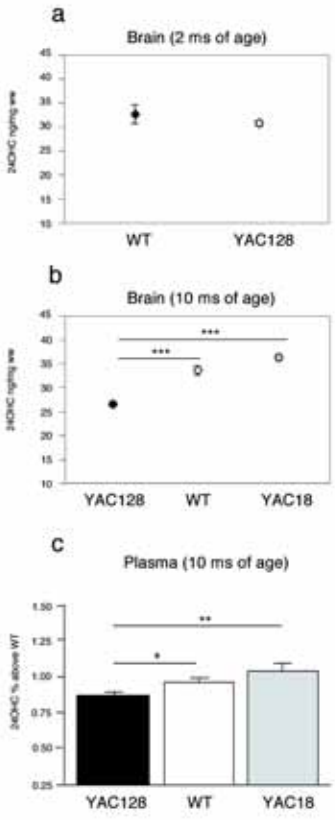

Figure 6

ABBREVATIONS

Huntington's disease (HD)

sterol regulatory element binding protein (SREBP)

Central Nervous System (CNS)

N-methyl-D-aspartic (NMDA)

yeast artificial chromosome (YAC)

3-hydroxy-methyl-glutaryl-CoA-Reductase (HMGCoAR)

24-S-hydroxycholesterol (24OHC)

mass spectrometry (MS)

blood-brain barrier (BBB)